Sherry Huang[1,2,3#], Christian Pfeiffer[2#], Jana Hollmann[2], Sebastian Friede[2], Justin Jin-Ching Chen[3], Andreas Beyer[2], Benedikt Haas[2], Kerstin Volz[2], Wolfram Heimbrodt[2], Jose Maria Montenegro Martos[2*], Walter Chang[3], and Wolfgang J.Parak[2*]

[1] Institute of Polymer Science and Engineering, National Taiwan University, Taipei, Taiwan

[2] Fachbereich Physik and WZMW, Philipps Universität Marburg. Marburg, Germany

[3] Department of Biomedical Engineering, Chung Yuan Christian University, Chungli, Taiwan

[#]both authors contributed equally to this study

[*]corresponding authors: wolfgang.parak@physik.uni-marburg.de

jose.montenegromartos@physik.uni-marburg.de

Synthesis and characterization of colloidal fluorescent silver nanoclusters

Supporting Information

SI.1: Synthesis of small, fluorescent silver nano clusters (Ag NCs)

SI.2: Purification and characterization of fluorescent silver nanoclusters

SI.3: Interaction of silver nanoclusters and cells

SI.1: Synthesis of small, fluorescent silver nano clusters (Ag NCs)

SI.1-1: Chemicals

Didodecyldimethylammonium bromide (DDAB, ≥98% purity; Fluka), decanoic acid (≥98% purity; Aldrich), tetrabutylammonium borohydride (TBAB, 98% purity; Aldrich), silver chloride (AgCl, 99.9%-Ag purity; Strem chemicals), (±)-α-lipoic acid (≥99% purity; Sigma), 10 nm Au NP (British Biocell International).

SI.1-2: General description

We introduce a general route to prepare small silver nanoclusters (Ag NCs) in organic phase. This synthesis is based on a previously reported synthesis of gold nanoclusters (Au NCs).[1] First, bigger silver nanoparticles (Ag NPs) were synthesized. Their size distribution was improved by an etching step via further addition of AgCl precursor solution. By adding freshly reduced lipoic acid to the Ag NPs, the surfactant molecules on the etched NCs were replaced because of the stronger dithiol-Ag bonds. With this ligand exchange, small fluorescent Ag nanoclusters (Ag NCs) were obtained, not showing the typical plasmon peak at 430 nm as the Ag NPs do. This ligand exchange also allowed the Ag NCs to become water-dispersible by deprotonation of the lipoic acid under basic conditions.

SI.1-3: Synthesis of small silver nanoparticles in toluene (Ag NPs)

All precursor solutions were freshly prepared. The silver precursor solution was a transparent and colorless solution of 25 mM AgCl in 100 mM didodecyldimethylammonium bromide (DDAB) in toluene. The dissolving needed some hours and had to be done protected from light. Also a 25 mM DDAB solution in toluene was prepared. Furthermore solutions of 100 mM decanoic acid in 25 mM DDAB in toluene and 100 mM tetrabutyl-ammoniumborohydride (TBAB) in 25 mM DDAB in toluene were prepared.

First, 156.3 µL of the decanoic acid solution, 200 µL of the AgCl solution and 250 µL of the TBAB solution were mixed and stirred for 10 minutes at RT in a small glass vial. The solution turned light brown immediately after mixing the solutions, which indicated the formation of Ag NPs. An etching step was necessary to improve the Ag NPs size distribution. For this etching step, 2500 µL of the AgCl solution were added by adding one drop each three seconds to the Ag NPs reaction mixture and stirring it for 10 minutes at RT. During the addition the solution was getting darker brown to almost black. During this procedure the plasmon peak of the Ag NPs first started to grow and then stabilized, which could be detected by UV/vis spectra (Figure S1). At the beginning, the plasmon resonance peak at 430 nm was weak, increased by adding the first µL of AgCl solution and slightly decreased during the further addition of AgCl solution.
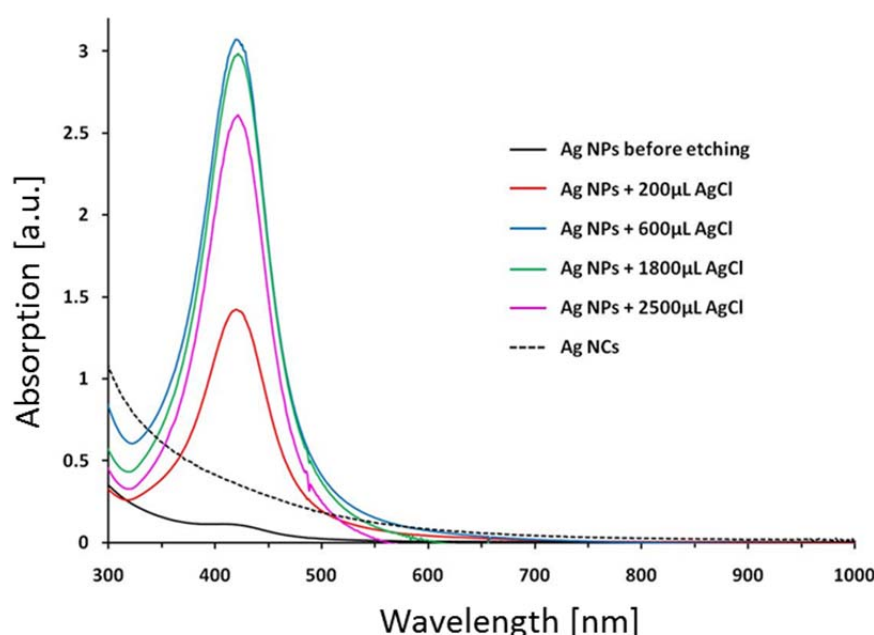

Figure S1: UV/vis absorption spectra of Ag NPs before etching (black line), Ag NPs during the etching step (colored lines) and Ag NCs (dashed line). The absorption spectra have been corrected for dilution effects upon addition of AgCl solution.

SI.1-4: Ligand exchange with Lipoic acid (Ag NCs)

For the ligand exchange, it was very important that the solutions of lipoic acid and TBAB were freshly prepared and mixed. The lipoic acid solution was 200 mM in 25 mM DDAB in toluene and the TBAB solution was 50 mM in 25 mM DDAB in toluene. The mixture of both solutions led to the reduction of lipoic acid to dihydrolipoic acid (DHLA) that bound to the Ag NCs through the free generated thiol groups.

1600 µL of both lipoic acid and TBAB solutions were mixed and stirred ca. 5 minutes before the synthesis of the Ag NPs was finished. The freshly prepared small Ag NPs were added to the mixture under vigorous stirring one drop every three seconds in a small closeable glass vial. During this process the Ag NCs started to precipitate. After adding the Ag NCs to the freshly reduced lipoic acid (DHLA) the reaction was stirred for 10 minutes at RT and was afterwards divided into four lockable vials. These vials were exposed to UV light with a wavelength of 336 nm for 10 minutes. Then each vial was gently shaken and exposed for another 10 minutes. The vials were heated at 70 °C for one minute. After this, the vials were again exposed to UV light for 10 minutes, gently shaken and again exposed for 10 minutes. Afterwards all Ag NCs should be aggregated and stuck to the wall of the vials. If this was not the case the exposure, shaking and heating process needed to be repeated until the clusters stuck to the wall. The yellowish solution was trashed. Then, the Ag NCs were dissolved in methanol and pooled. Afterwards the methanol was removed under reduced pressure with a rotary evaporator at 40 °C. To remove excess ligands 2 mL of chloroform were added to the Ag NCs and gently shaken. The solvent was discarded afterwards. The clusters were re-dissolved in methanol and dried under reduced pressure at 40 °C. Afterwards the clusters were dissolved in SBB9 (50 mM sodium borate buffer, pH 9), which deprotonated the lipoic acid and allowed the clusters to be dispersible in water. The dispersed clusters were heated overnight at 55 °C. The purification of the clusters started passing them through a syringe membrane filter (0.22 µm pore size) to remove remaining particle aggregates. By passing through a 100 kDa and 30 kDa MWCO centrifuge filter membrane the smaller particles were separated from the bigger ones. The small clusters were at the end concentrated and collected by a 3 kDa MWCO centrifuge filter.

SI.2: Purification and characterization of fluorescent silver nanoclusters

SI.2.1: Purification by gel electrophoresis

It was possible to purify the Ag NCs from impurities like unbound ligands or bigger clusters by gel electrophoresis. For this purpose a gel of 2% agarose and 0.5 M Tris-borate-EDTA (TBE) was prepared and placed into an electrophoresis chamber filled with 0.5 M TBE. The loading buffer was supplemented with Orange G. The field intensity was 10 V·cm^{-1} and the electrophoresis was run for one hour. As reference a sample of 10 nm Au NPs coated with bis(p-sulfonatophenyl)phenylphosphine (from BBI) [2] was used for comparison, see Figure S2. Then, the labeled area in Figure S2 was cut out and placed into a dialysis membrane (MWCO 50 kDa) and placed for another 20 minutes into the chamber at 10 V·cm^{-1}, which extracted the clusters out of the gel. Afterwards the cluster solution was concentrated by a 3 kDa centrifuge filter. Figure S2 shows that the clusters are much smaller than the 10 nm gold particles. Orange G was removed from solution via concentration with the centrifuge filters.
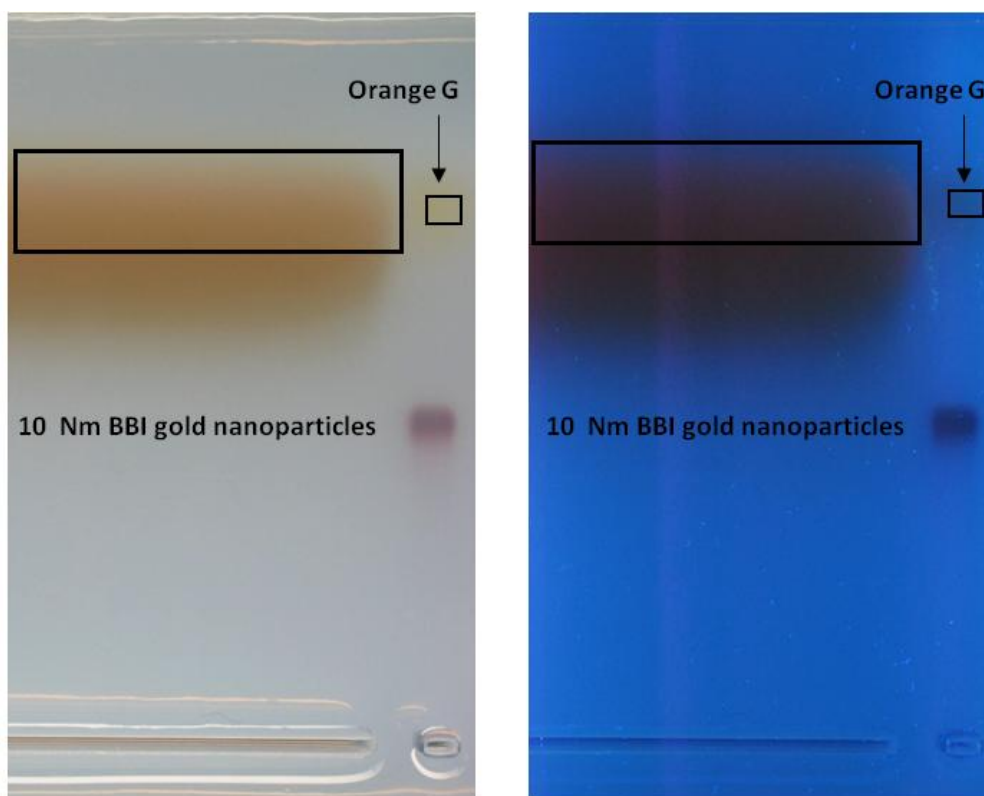

Figure S2: Gel electrophoresis of Ag NCs (2% Agarose, 10 V·cm^{-1}, 1 h) under visible (left) and UV light (right). The labeled part was cut out of the gel and the NCs were extracted.

SI.2.2: Purification by high performance liquid chromatography (HPLC)

A second purification was carried out using a HPLC system in order to remove any excess of ligands present in the sample. For this purpose an Agilent 1100 HPLC System was used including a self packed column filled with Sephacryl S300HR. As mobile phase a mixture of 50 mM sodium borate buffer with a pH value of 9 and 0.1 M sodium chloride (SBBS9) was used. The flow was set to 1.0 mL·min^{-1}. The fraction between 79 to 94 min was collected containing the fluorescent Ag NCs. The chromatogram is shown in Figure S3.
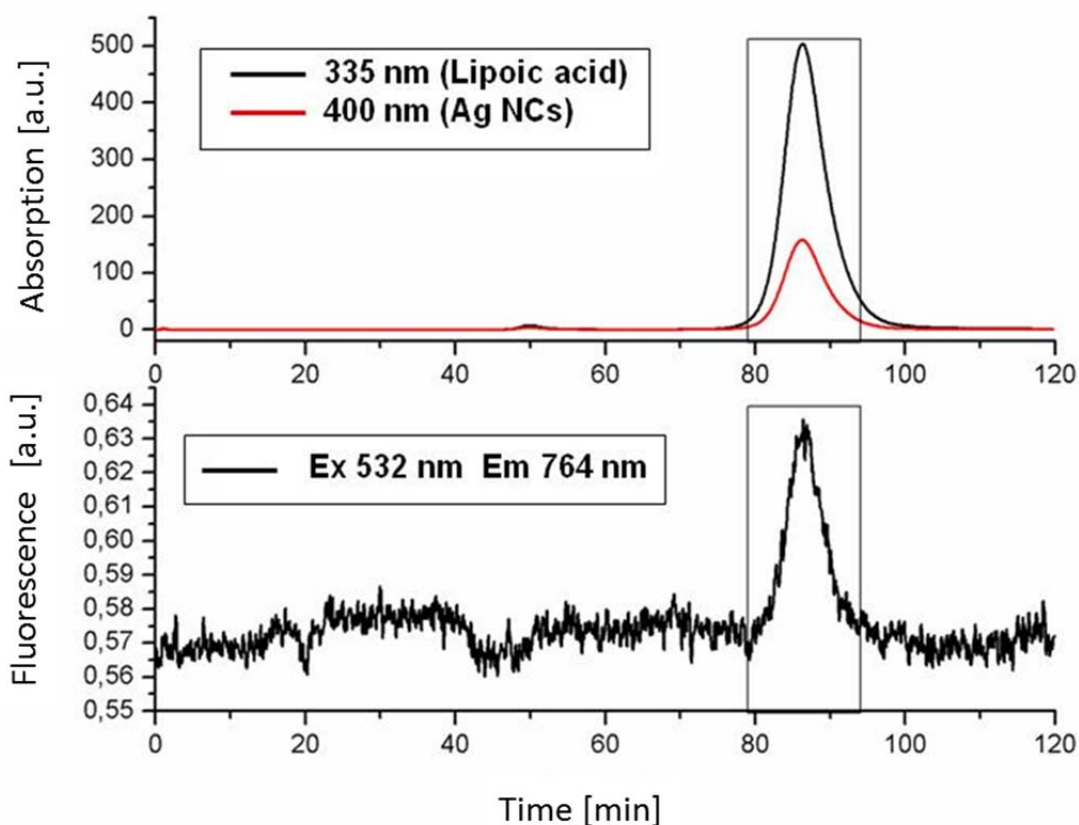

Figure S3: HPLC of Ag NCs (SBBS9, 1 mL·min^{-1}, Sephacryl S300HR). The clusters were eluted between 79 and 94 minutes during this time period an increase of the fluorescence was detected. Absorption was recorded at 335 nm and 400 nm where lipoic acid, and the Ag NCs absorb, respectively. Emission of the Ag NCs was recorded at 764 nm with 532 nm excitation.

SI2.3: Characterization by UV/vis spectroscopy

UV/vis spectra were measured by an Agilent 8453 spectrometer. In Figure S1 the plasmon resonance peak of the Ag NCs is not present after the ligand exchange with DHLA. During the etching step, the size of the peak first increased upon addition of the Ag precursor, which is an indication for an increasing size of the Ag NPs. By adding more of the silver precursor solution the peak stabilized, which is sign for a having reached a more monodisperse distribution of the NPs. After the ligand exchange the size of the Ag NCs decreased that much

that a plasmon resonance peak was not present any more. All the spectra were corrected for the dilution effects during adding AgCl solution.

SI2.4: Characterization of Ag NCs by dynamic light scattering (DLS) and laser Doppler anemometry (LDA)

The determination of the hydrodynamic diameter and zeta-potential was carried out by Dynamic Light Scattering (DLS) and Laser Doppler Anemometry (LDA) using a Malvern zetasizer nano device. In Figure S4, the DLS distribution of the Ag NCs is shown. The average hydrodynamic diameter of the NC was measured to be 2.7 nm. The zeta-potential was detected to be -30 ± 2 mV, which is an indicator for high colloidal stability.
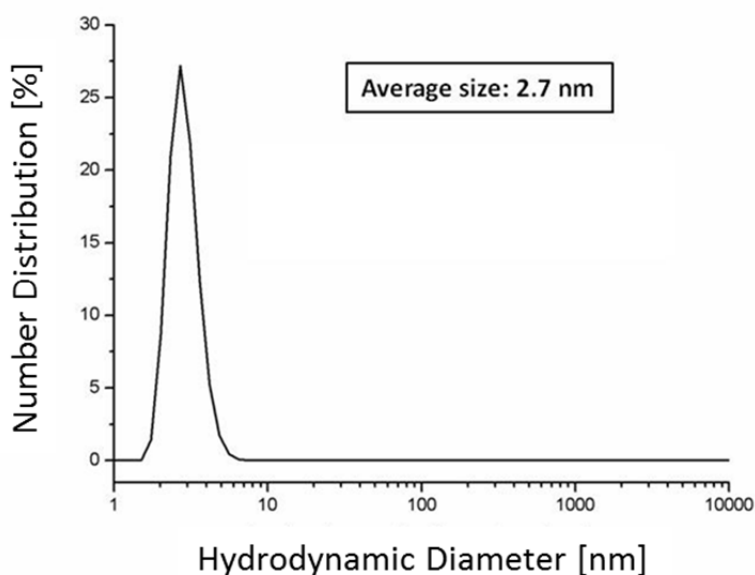

Figure S4: Number distribution N of hydrodynamic diameters of Ag NCs in SBB9 as determined with DLS. The Ag NCs average hydrodynamic diameter is 2.7 nm.

SI.2.5: Characterization by transmission electron microscopy (TEM)

For TEM measurements a JEOL JEM-3010 was used. In Figure S5 the particles are shown with 200k magnification. The copper grids were prepared by placing one drop of the particle dispersion on top of the grid and drying at RT over night. The grids have to be protected from dust while drying. Before the etching step the particles (Ag NPs) are highly polydisperse (Figure S5 A). Most of the particles have a diameter of ca. 4 nm, but there are also particles with a size between 10 nm and even more than 30 nm. After the etching step the size distribution is relatively monodisperse with a size of 4.8 ± 0.8 nm, see Figure S5 B This demonstrates that the bigger particles got etched, whereas the smaller particles increased in size during this step. The final size of the clusters of 2.2 ± 0.2 nm was reached after the ligand

exchange and phase transfer with DHLA (Figure S5 C). This result is in good agreement with the DLS results.
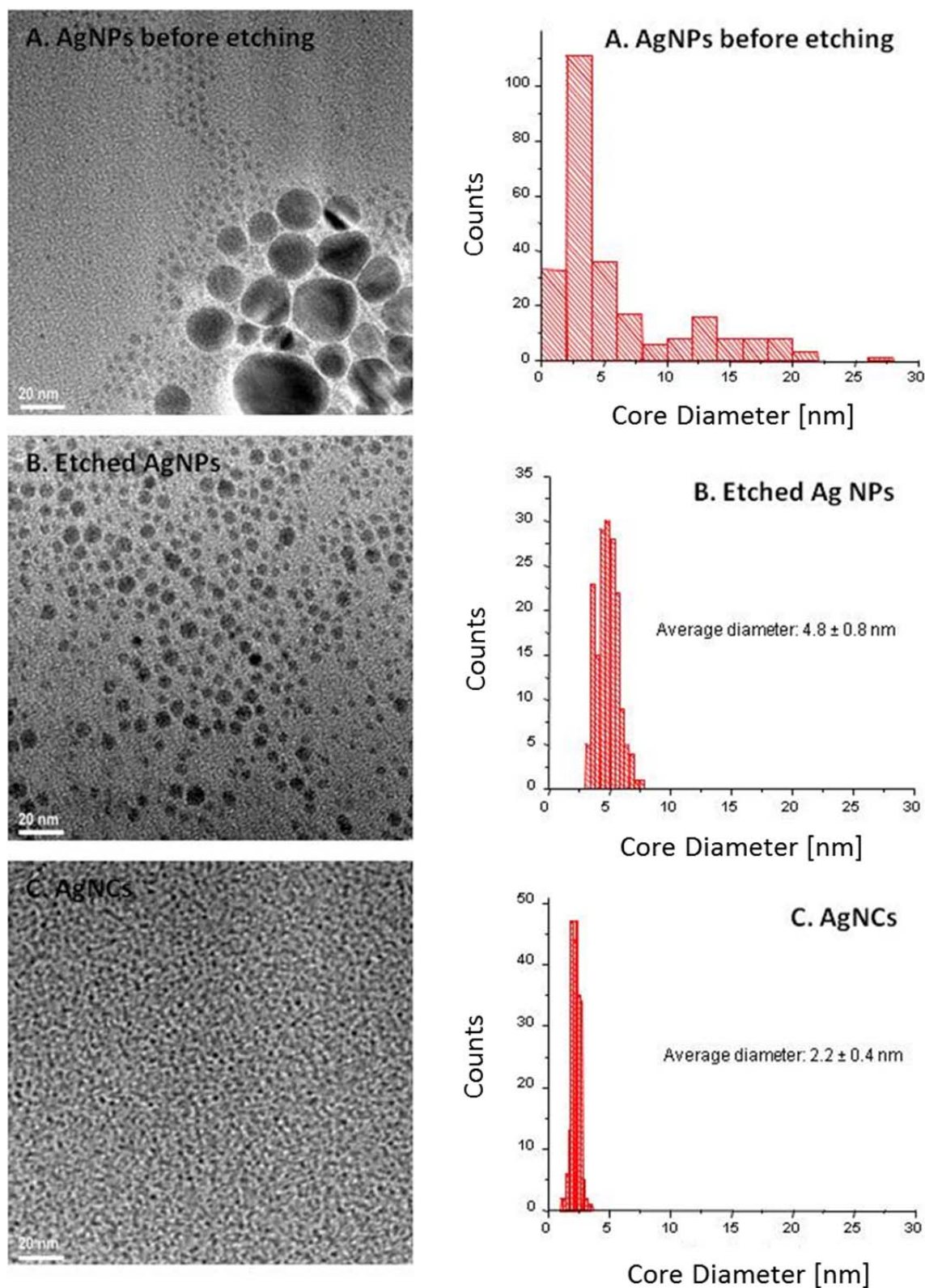

Figure S5: TEM images histograms of the size distribution of Ag NPs before etching (A), Ag NPs after etching (B) and Ag NCs after ligand exchange (C). The scale bar is 20 nm at a magnification of 200k.

In Figure S6 and S7 high resolution TEM pictures of a mixture of Ag NPs and Ag NCs are shown. The big picture (A) in Figure S6 shows an overview over some small and big particles whereas the small pictures show a more detailed view of a small NC and a big NP (B) and the fast Fourier transformation FFT of the big NPs (C). In Figure S7 the FFT of a small NC is show, in which the reflexes of the Ag {111} lattice planes can be seen. The image also displays a linescan along the NC. The fringe distance corresponds to Ag {111}. From this, it becomes clear that only Ag can explain the diffraction as well as the lattice spacing of the clusters:[3, 4]

Ag: {111} 4.319   {002} 4.988

AgCl: {111} 3.123   {002} 3.606   {022} 5.100

Ag$_2$O {011} 2.997   {111} 3.671   {002} 4.239   {112} 5.192
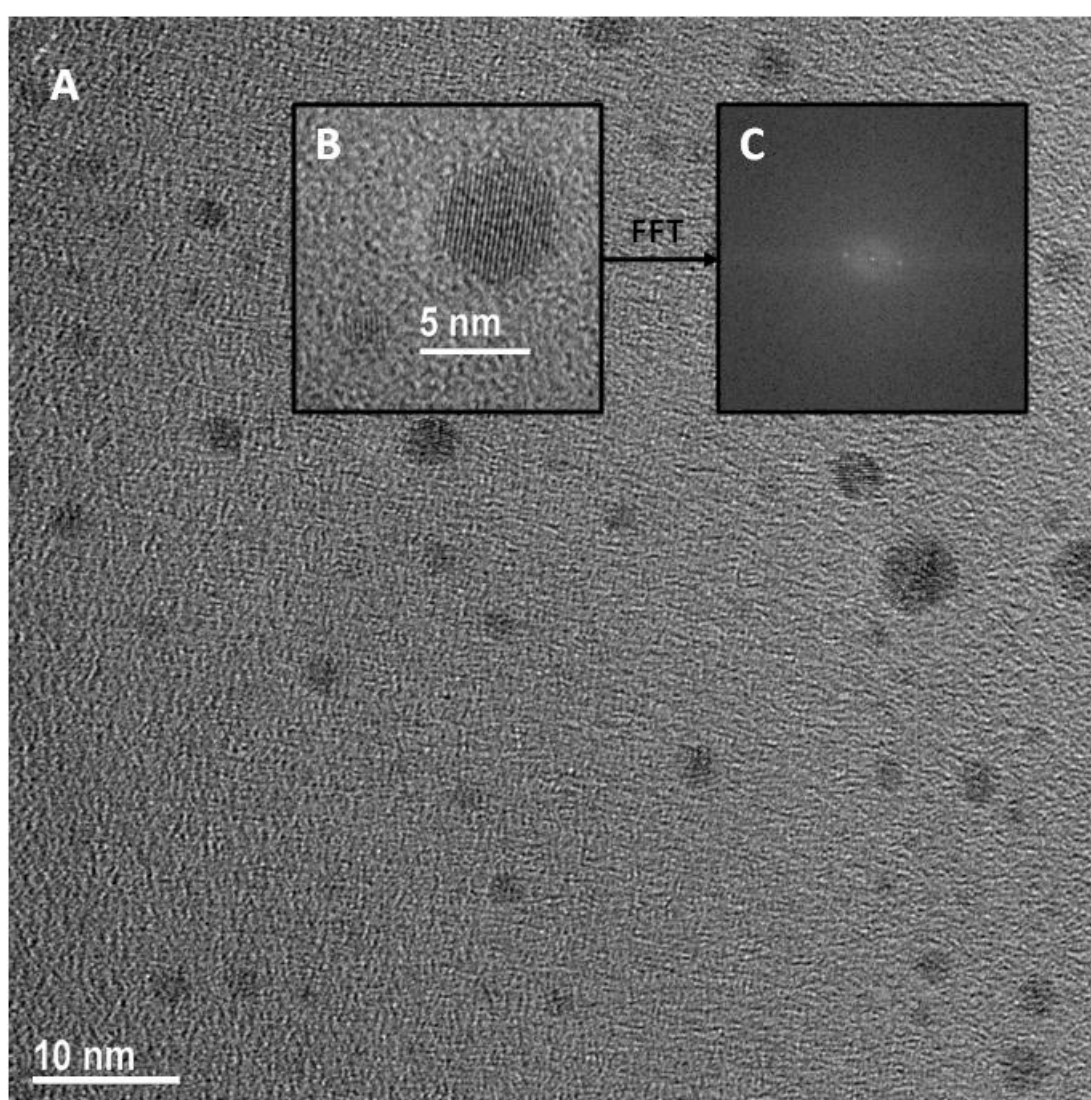

Figure S6: High resolution TEM picture of a mixture of Ag NPs after etching and Ag NCs. The images shows an overview (A), a detail view of a big particle (above the scale bar) and a small particle (left to the scale bar) (B), and a fast Fourier transformation of the big particle (C).
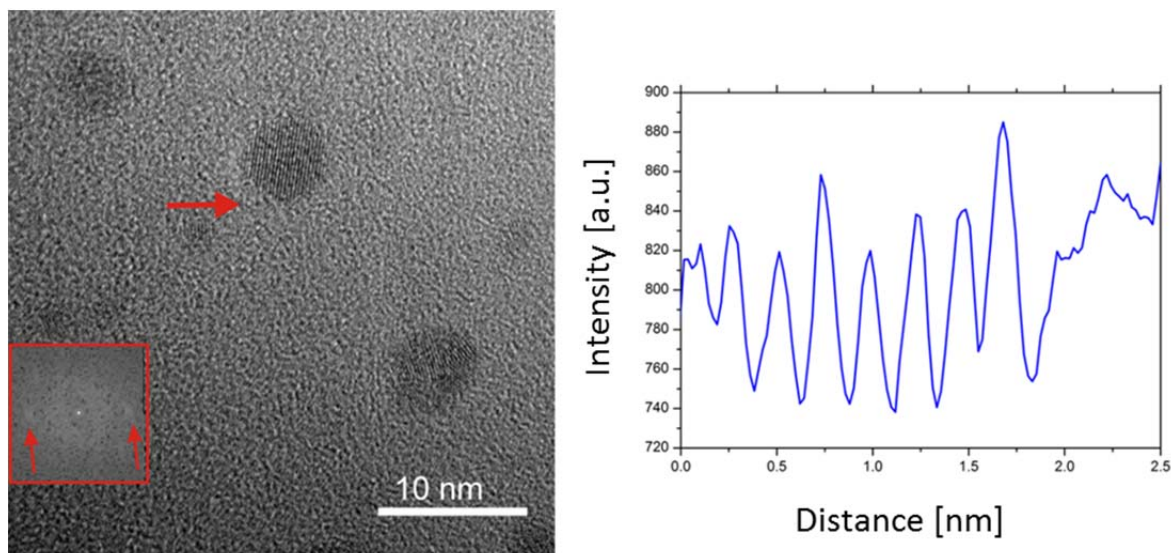
Figure S7: High resolution TEM picture of a mixture of Ag NPs after etching and Ag NCs. The images show an overview, with the fast Fourier transformation of one small NC as inset. On the right a linescan across the NC (as indicated by the red arrow) is shown.

SI.2.6: Quantum yield

The quantum yield (QY) of the Ag NCs was calculated by the method described by Lakowicz.[5] As reference dye quinine sulfate in 0.1 M sulfuric acid ($\Phi = 0.577$) was used. In order to compare the QY of the Ag clusters with the dye the integrated fluorescence intensity at emission at 410 nm was plotted versus the absorbance at 410 nm. The plots are shown in Figure S8. The quantum yield of the Ag NCs was calculated to be $2.4 \cdot 10^{-4} = 0.024\%$.
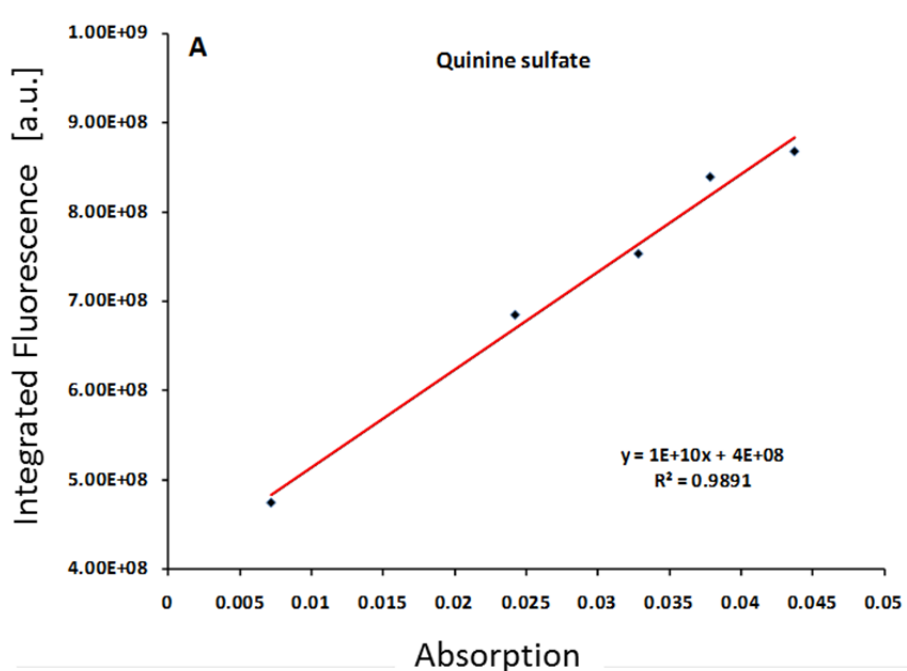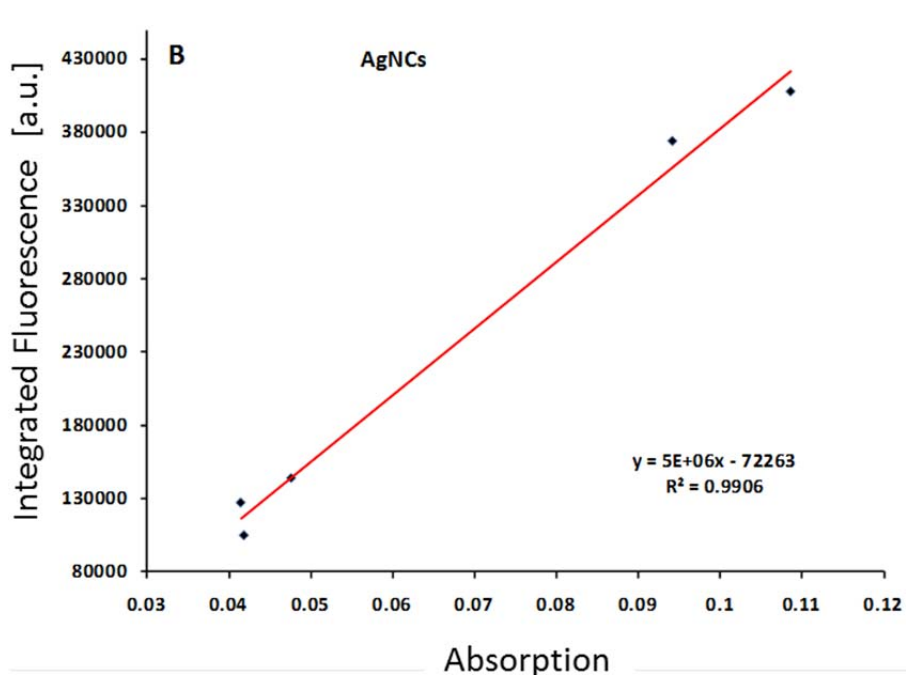
Figure S8: Plot of the integrated fluorescence intensity of the emission at 410 nm versus the absorbance at 410 nm for quinine sulfate in 0.1 M H_2SO_4 (A) and Ag NCs in SBBS9 (B).

SI.2.7: Laser-excited photoluminescence (PL) and time resolved photoluminescence (trPL)

The samples were transferred into Hellma® Quartz SUPRASIL® precision cells (104.002F-QS) to perform PL and trPL measurements. The precision cells were cleaned by soaking them overnight in 1% HELLMANEX® III solution. Subsequently the cells were flushed with pure water and deposited into acetone. Finally the cells were dried in a stream of pure nitrogen. A spectroscopic check of the empty cells was performed, using the same setup as for the experiments on the samples, to prove the cleanness of the cells. No PL signal was detectable in case of unfilled pure cells.

To excite the samples optically a pulsed Nd:YAG (neodymium-doped yttrium aluminum garnet) laser (Quantel Brilliant) was used accomplished with a 2nd Harmonic Generation Module (HGM). The excitation wavelength was 532 nm (2.33 eV). The pulses had a temporal full width at half maximum of about 4 ns. The emitted PL was collected by a lens system and focused on the entrance slit of a 0.25 m spectrograph (LOT, MS257™). In front of the entrance slit an optical longpass filter was mounted with an edge wavelength of 550 nm (OG550). For all PL and trPL measurements the width of the slit was 200 μm. The used grating had 300 lines/mm and a blaze wavelength of 500 nm. The grating-dispersed PL was detected by a silicon-based intensified charge-coupled device (ICCD) detector system (Andor iStar) with a minimal time resolution of 2 ns, given by the integration time window. The binning mode of the ICCD was set to full vertical for all measurements. Both, PL and trPL measurements were performed at room temperature.

For the PL measurements the integration time window was set to 1.1 μs. The number of averaging cycles was 300 for each measurement. In case of the Ag NPs, only an extremely

weak signal could be revealed. The PL could not be seen by the naked eye. In case of the Ag NCs, however, a pronounced red PL band with the maximum at about 1.82 eV (690 nm) was seen. The PL is actually bright and can be easily detected by the naked eye. The spectrum is depicted in Figure S9 and compared to the weak signal of the large Ag NPs.
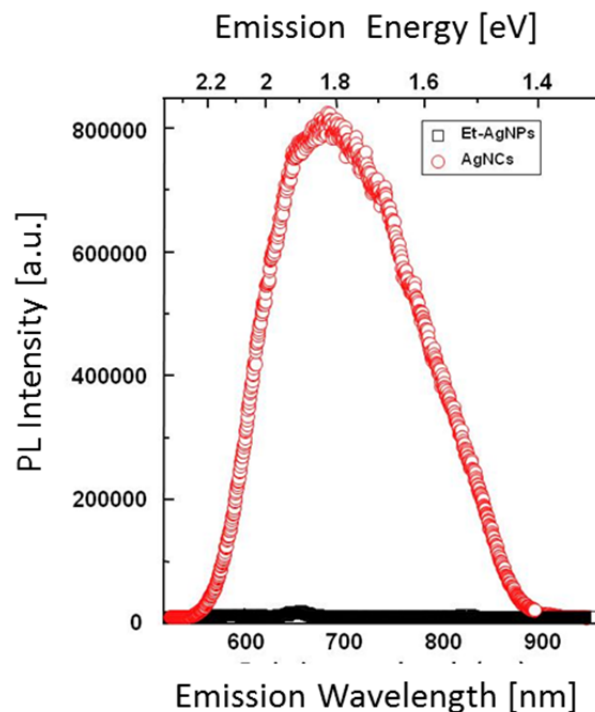

Figure S9: Comparison of the photoluminescence of etched Ag NPs (black squares) and Ag NCs (red circles).

The red PL of the NCs had a maximum at 678 nm (1.83 eV) and a rather big full width at half maximum of about 200 nm. In Figure S10 the transient of the strong red PL band is given. The decay curve exhibits a strong non-exponential behavior with decay times varying from about 200 ns in the beginning up to about 3 µs at later times. Such long lifetimes are typically for forbidden electronic transition with only small dipole-matrix-elements. In the present case the transition is most likely due to a spatially indirect transition from excited electrons in the LUMO state with the positively charged silver particle. The quantum confined splitting and blue shift of the particle states enables such transitions if the particle size is small enough.
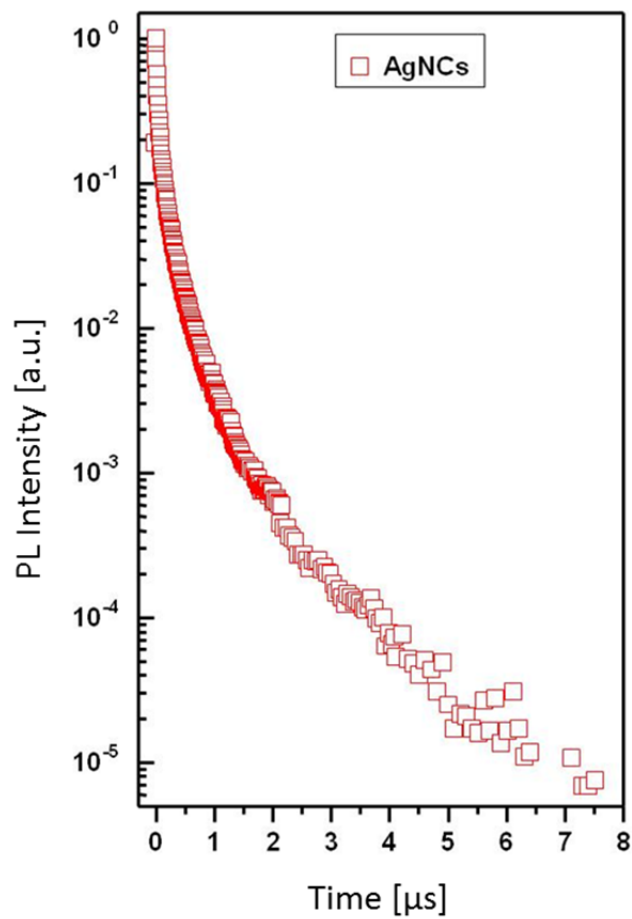
Figure S10: Transient of the strong red photoluminescence band of the Ag NCs.

SI.3: Interaction of silver nanoclusters and cells

SI.3.1: Cell culture

MCF-7 human breast cancer cells were maintained in T-75 flasks (Falcon, Heidelberg, Germany) in Eagle's minimum essential medium (EMEM) supplemented with 10% fetal bovine serum (FBS), 100 IU mL^{-1} penicillin, 100 IU mL^{-1} streptomycin, and 0.01 mg mL^{-1} bovine insulin at 37 °C, 5 % CO$_2$, and 95% relative humidity. The cells were trypsinized with 0.25% trypsin/EDTA solution and subcultured in the growth medium for further studies.

SI.3.3: Cytotoxicity assay

One also might argue that due the fact that Ag NCs contain an intrinsically cytotoxic element (Ag) they are (even in case of higher quantum yields) of no practical use for cellular labeling. In order to use the fluorescent Ag NCs in biological applications we determine their cytotoxicity. After trypsination MCF-7 cells were seeded in 96 well plates with a density of 10^4 cells per well and incubated for 24 hours. The growth medium was replaced by medium containing Ag NCs. As maximum concentration this medium contained 80% growth medium and 20% of Ag NC solution with an optical density (OD) at 400 nm of 25, which corresponds to 0.48 mg/mL or 14 µM Ag NCs.[1] Solutions with lower Ag NC concentration were obtained by dilution. Cells were incubated at 37 °C, 5% CO$_2$, and 95% relative humidity for 6 or 24 hour in the Ag NC containing medium. The cytotoxicity of the Ag NCs was evaluated using the CellTiter-Blue cell viability assay. Quantification was made by measuring the absorbance at 570 nm with a spectrophotometer (ELISA reader). Date are displayed in Figure S11. The preliminary cytotoxicity data suggest, in case of low Ag NC concentrations, that only limited cytotoxicity is provoked (*cf.* Figure 3). Thus cytotoxic effects for experiments with cell cultures over limited periods of times are tolerable. We believe that capping of the Ag NCs with lipoic acid reduces release of Ag$^+$ ions from their surface.

---

[1] The Ag concentration was measured by the inductively coupled plasma atomic emission spectrometer (ICP-AES; HORIBA JOBIN-YVON-JY2000 2). For an Ag concentration of 83.087 µg/mL the OD$_{400}$ of Ag NCs was determined to be A = 0.865. The concentration of Ag NCs in the solution is therefore: c(Ag) = 83.087 µg/mL / $3.54 \cdot 10^4$ g/mol = 2.35 µM. Hereby the molecular mass of one Ag NC (under neglectance of the DHLA capping) was estimated from the density of Ag (ρ = 10.5 g/cm^3) and the volume of each Au NC as calculated from the diameter determined by TEM (V = 4/3 π (d/2)^3 = 4/3 π (2.2 nm / 2)^3 = 5.6 nm^3) to M = $\rho \cdot$V$\cdot 6.02 \cdot 10^{23}$ mol^{-1} = 10.5 g/cm^3 $\cdot$ $5.6 \cdot 10^{-21}$ cm^{-3} $\cdot$ $6.02 \cdot 10^{23}$ mol^{-1} = $3.54 \cdot 10^4$ g/mol. As the molar mass of one Ag atom is 107.89 g/mol one Ag NC with a molar mass of $3.54 \cdot 10^4$ g/mol comprises $3.54 \cdot 10^4$ g/mol / 107.89 g/mol $\approx$ 330 Ag atoms. For an Ag concentration of 68.757 µg/mL the OD$_{400}$ of the Ag NCs was determined to be 0.716. This corresponds to a concentration of Ag NCs of c(Ag) = 68.757 µg/mL / $3.54 \cdot 10^4$ g/mol = 1.94 µM. According to the Beer-Lambert law the absorption is the product of the molar extinction coefficient ε, the concentration c, and the pathlength l, which was in the present case l = 1 cm: A = ε c l $\Rightarrow$ ε = A / (c·l). Thus ε(@400 nm) is the mean value of 0.865 / (2.35 µM·cm) and 0.716 / (1.95 µM·cm) = $3.68 \cdot 10^5$ M^{-1}cm^{-1}.
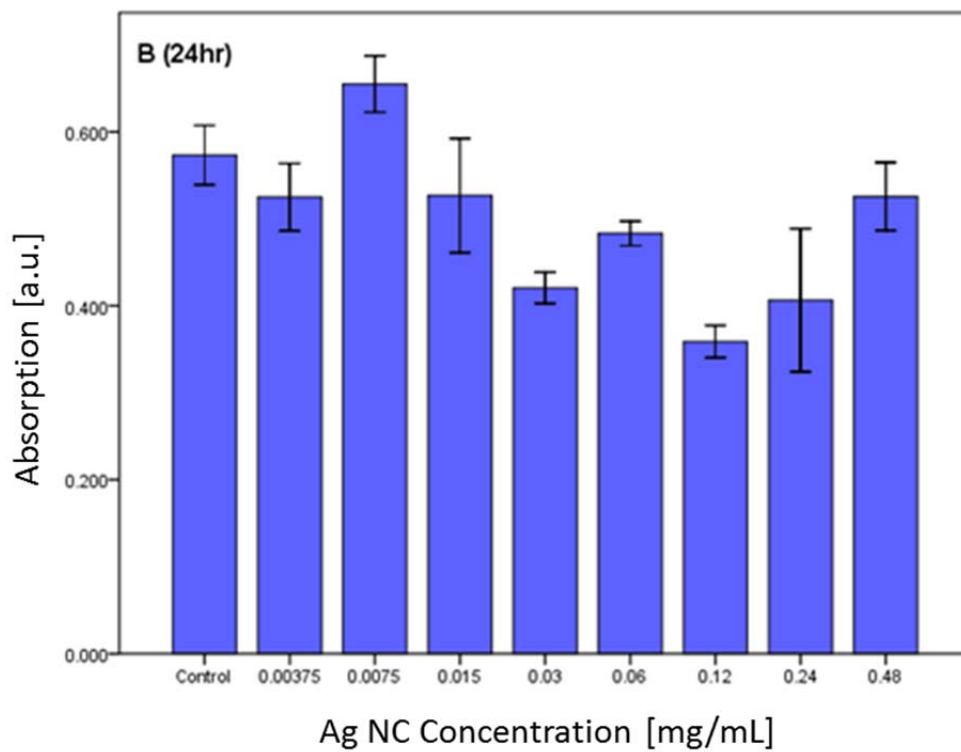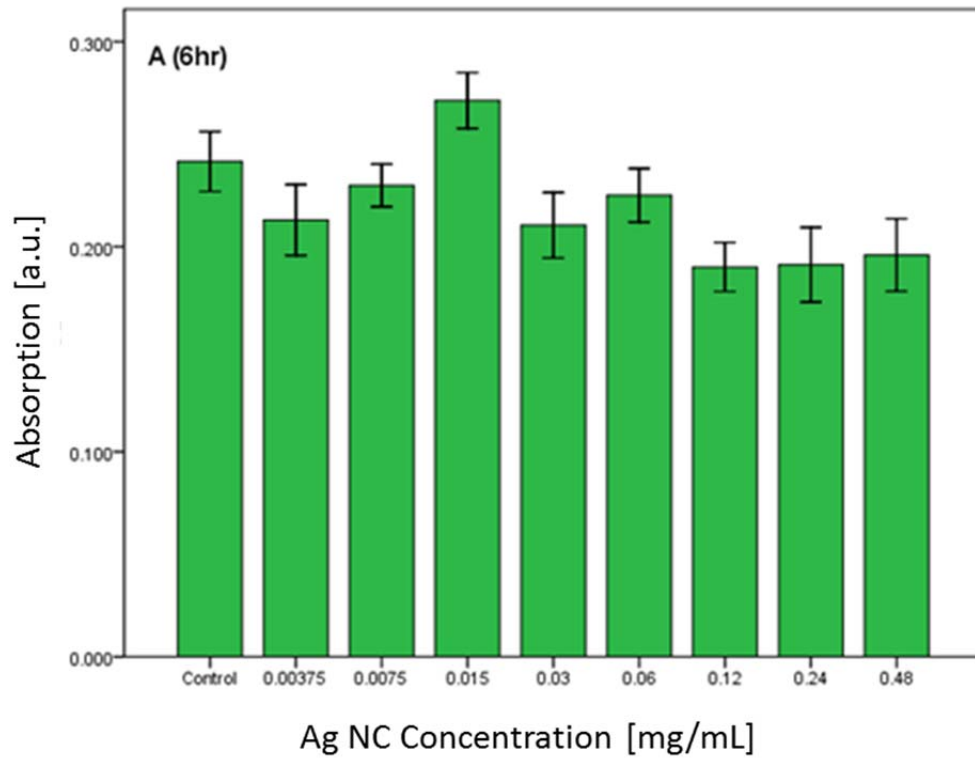
Figure S11: Cell viability assay using the CellTiter-Blue reagent with MCF-7 cells exposed to Ag NCs with serial dilutions for (A) 6 or (B) 24 hours. As read-out the OD at 570 nm is displayed. The results are represented as mean values ± standard error of the mean and were analyzed statistically using one-way ANOVA followed by Scheffé's test using SPSS version 17.0 to establish the significance of any differences. The level of statistical significance was set at p < 0.05.

SI.3.3: Uptake of silver nanoclusters by cells

To further explore the uptake of Ag NCs by living cells microscopy images of cells exposed to Ag NCs were recorded. After trypsination MCF-7 cells were seeded into 8-well coverglass chamber slides (Nunc, Roskilde, Denmark) with a density of 10^4 cells per well and incubated for 24 hours. The growth medium was replaced by medium containing Ag NCs. As maximum concentration this medium contained 80% growth medium and 20% of Ag NC solution with an optical density (OD) at 400 nm of 25, which corresponds to 0.48 mg/mL or 14 μM Ag NCs. Cells were incubated at 37 °C, 5% CO_2, and 95% relative humidity for 6 hours. Afterwards cells were stained with Hoechst 33342 for 30 min and then the cells were washed with PBS twice. The PBS was replaced with phenol red free EMEM medium containing 10% FBS, 100 IU mL^{-1} penicillin, 100 IU mL^{-1} streptomycin, and 0.01 mg mL^{-1} bovine insulin. Fluorescence images were acquired using a Zeiss laser scanning confocal microscope LSM510 with Plan-Neofluar 63×/1.4 NA Oil DIC objective, and the Axiovision 4.3 software Results are shown in Figure S12 and S13. Differential interference contrast (DIC) images show the colonies of MCF-7 cells. Fluorescence images of cells show the red fluorescence of Ag NCs throughout some cells and the blue-colored Hoechst33342 dye inside the nuclei. Thus Ag NCs were associated to cells.[1] Fluorescence imaging demonstrated that Ag NCs could be distinguished from background autofluorescence. It is important to point out, that in the case of our Ag NCs signal comes from fluorescence. This has to be clearly distinguished from scattering, which is often used for the imaging of larger metal NPs.[6-8] Fluorescence and scattering processes can be easily distinguished by time resolved measurements. Whereas the characteristic times of scattering processes used to be well below fs our fluorescence processes shows a decay in the microsecond range, *cf.* Figure 2b. It is obvious, therefore, that the images of the cells are due to fluorescence of the Ag NCs. However, fluorescence intensity was so weak that we could not clearly localize the Ag NCs and thus can not claim that they have been incorporated by the cells. In particular no distribution in intracellular vesicular structures could be observed, as this had been in the case of Au NCs.[9]
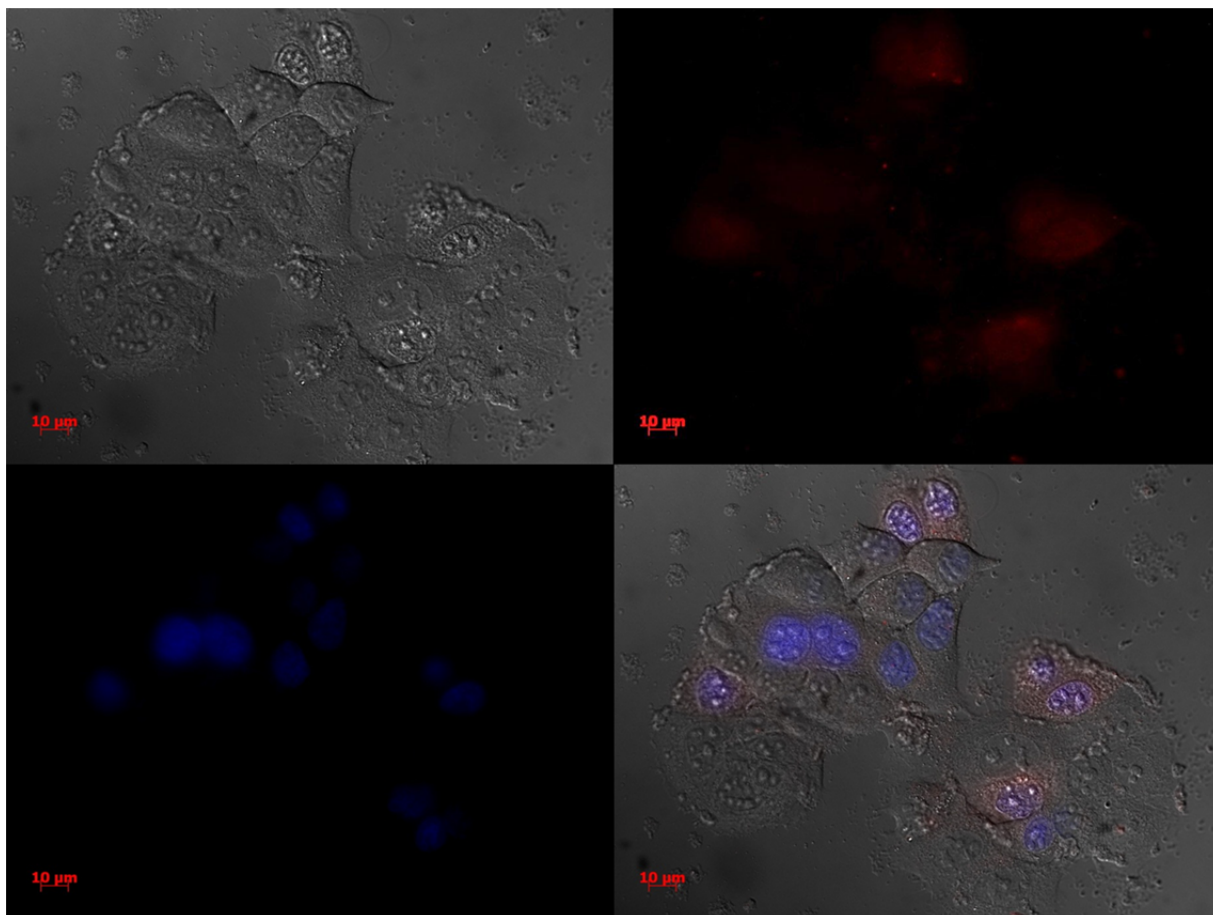
Figure S12: Fluorescence microscopy image of live MCF-7 cells after 6 hours of incubation with Ag NCs. (A) Differential interference contrast (DIC) image, (B) red fluorescence signal of Ag NCs, (C) blue fluorescence signal of Hoechst 33342, (D) merged picture of A, B, and C. Scale bars represent 10 μm.
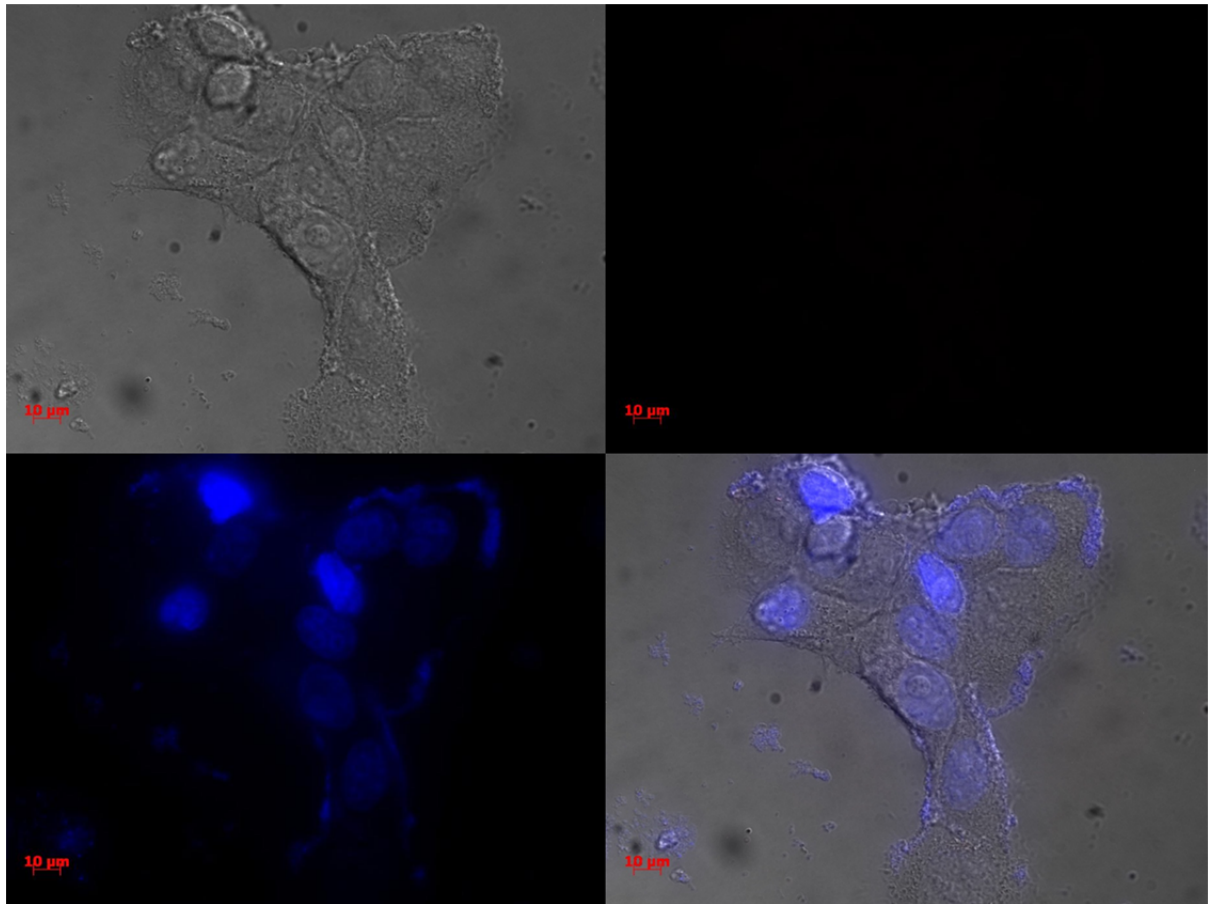
Figure S13: Fluorescence microscopy image of live MCF-7 cells without added Ag NCs as control, recorded with the same settings as shown in Figure S12. (A) Differential interference contrast (DIC) image, (B) red fluorescence signal, (C) blue fluorescence signal of Hoechst 33342, (D) merged picture of A, B, and C. Scale bars represent 10 μm.

References

(1)   Lin, C. A. J.; Yang, T. Y.; Lee, C. H.; Huang, S. H.; Sperling, R. A.; Zanella, M.; Li, J. K.; Shen, J. L.; Wang, H. H.; Yeh, H. I.; Parak, W. J.; Chang, W. H., *ACS Nano* **2009,** *3*, 395-401.

(2)   Zanchet, D.; Micheel, C. M.; Parak, W. J.; Gerion, D.; Alivisatos, A. P., *Nano Lett.* **2001,** *1*, 32-35.

(3)   Hull, S.; Keen, D. A., *Phys. Rev. B* **1999,** *59*, 750-761.

(4)   Niggli, P., *Z. Kristallogr.* **1922,** *57*, 253-299.

(5)   Lakowicz, J. R., *Principles of Fluorescence Spectroscopy*. Third Edition ed.; Springer: New York, 2006; p 954.

(6)   Jin, R.; Cao, Y.; Mirkin, C. A.; Kelly, K. L.; Schatz, G. C.; Zheng, J. G., *Science* **2001,** *294*, 1901-1903.

(7)   Sonnichsen, C.; Geier, S.; Hecker, N. E.; von Plessen, G.; Feldmann, J.; Ditlbacher, H.; Lamprecht, B.; Krenn, J. R.; Aussenegg, F. R.; Chan, V. Z. H.; Spatz, J. P.; Moller, M., *Appl. Phys. Lett.* **2000,** *77*, 2949-2951.

(8)   Krpetic, Z.; Porta, F.; Caneva, E.; Santo, V. D.; Scarì, G., *Langmuir* **2010,** *26*, 14799-14805.

(9)   Parak, W. J.; Boudreau, R.; Gros, M. L.; Gerion, D.; Zanchet, D.; Micheel, C. M.; Williams, S. C.; Alivisatos, A. P.; Larabell, C. A., *Adv. Mater.* **2002,** *14*, 882-885.